Design of a Compact, Agile AUV with Large Thrust-to-Weight Ratio

1st Marc Hildebrandt
Underwater Robotics
DFKI
Bremen, Germany
marc.hildebrandt@dfki.de

***Abstract*—In this work the design and integration process of a small AUV system with a large thrust-to-weight ratio is described. The whole process from initial design considerations over electronic integration, manufacturing of non-COTS-components and testing of the system in a seawater basin is covered.**

***Index Terms*—AUV, small, fast, thrust-to-weight ratio, autonomous**

I. Introduction

This work aims to explore very small AUVs with a large thrust-to-weight ratio and under-actuated control mechanisms. The aspects of design, control, autonomy, navigation and usability was studied. Typical AUV systems have a relatively small thrust-to-weight ratio and consequently relatively low maximum speeds and accelerations. Typical values are 0,078 (100N/1275N) for the DeepLeng AUV [6] , 0,054 (16N/294N) for the Remus AUV [2] and 0,044 (120N/2698N) for the FlatFish AUV [1]. For this project the design of a AUV called ”Arrow” is proposed with a much larger thrust and significantly reduced weight, resulting in a thrust-to-weight ratio larger than 1. This significant increase in relative thrust should enable the vehicle to perform maneuvers impossible for other AUVs, which in turn could lead to a number of new applications.

II. State of the Art

There is very little publicly available published research on high thrust-to-weight ratio AUVs. There are two groups who published in this field: Virginia Tech [5] and KTH Royal Institute of Technology in Stockholm [3]. Their vehicles however stayed well below a thrust-to-weight ratio of 1. The older research from Virginia Tech consisted an AUV build for high speeds, leading to a large thrust-to-weight ratio but not focusing on complex motion. A specialty of their vehicle was the fact, that the vehicle was inherently negatively buoyant, requiring active propulsion to surface. This was done to increase maximum velocity by using earth’s gravitation to increase velocity on downward trajectories. The newer research from KTH focuses more on the aspect of hydrobatics, so underactuated underwater vehicle dynamics, their SAM AUVs do not feature thrust vectoring but change their attitude by shifting of internal weights, similar to an underwater glider. The vehicle’s maximum thrust could not be found in publications, but since it’s reported maximum velocity is 3m/s at a weight of approximately 20kg (14kg without battery), it is estimated that it features a thrust-to-weight ratio well below 1. Another area where a large thrust-to-weight ratio is a mere side-effect of the vehicle design are military torpedo systems, which could to some degree considered a type of AUV system. Most torpedo systems reportedly have a large top speed, often exceeding 20 m/s, leading to relatively large thrust-too-weight ratios. Since there is no publicly available research data on this type of vehicle and their scope and size is completely different from the design described here, further investigation into this military application systems is omitted.

III. Design

A number of design criteria have been set for the development process:

- maximizing thrust-to-weight ratio
- using a coaxial thruster to cancel roll movements
- a gimballed thruster allowing vectored thrust
- a hydrodynamic hull optimized for low drag at high velocities
- inclusion of basic sensors and control capabilities
- utilization of COTS components wherever possible
- iterative design process

A. Mechanical

The first component which needed to be selected was the propulsion system. With regard to budget, availability and size three different thruster systems were considered: T200 and T500 by BlueRobotics as well as the Diskdrive80 by Hydromea. The Diskdrive80 has a lateral cable outlet, which makes it hard to integrate into a streamline nozzle design. The T500 was selected due to its maximum thrust of 160N and ease of integration into a custom nozzle (see figure 1). Due to the similarities between the two thrusters from BlueRobotics, a second, smaller version of the vehicle was designed around the T200 thruster, resulting in the ”‘Arrow”’ and ”‘Arrow-Mini”’ vehicle designs depicted in 2.

Taking the outer diameter of the designed dual-thruster nozzle, a basic hydrodynamically optimized hull design was selected, resulting in the Arrow vehicle’s dimensions of 900mm length with a 160mm diameter and the Arrow-Mini with a length of 425mm and a diameter of 100mm. The next step was to fit a watertight housing into the hull design

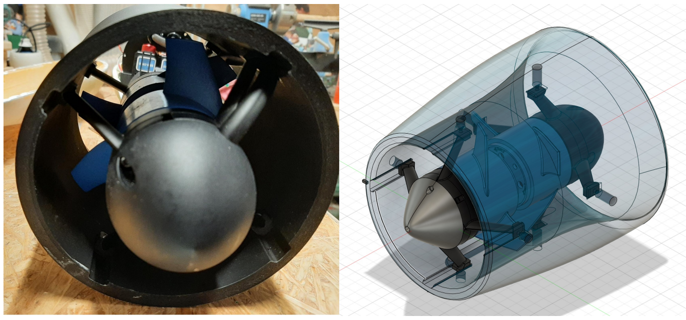

Fig. 1. Two BlueRobotics T500 thusters in a custom nozzle.

Fig. 2. First concept of AUV design as 3d prints.

and select a suitable power source. For both designs pressure housings from BlueRobotics were selected, a 300mm housing with 100mm diameter for the large vehicle, a 150mm housing with 50mm diameter for the small AUV. When selecting power sources it became clear that most of the housings would be occupied by batteries in order to be able to deliver the required power for a reasonable amount of time for experiments. A 22.2V 16kAh battery was selected for the large vehicle and a 14.8V 4.4kAh battery for the small AUV. This would result in an endurance of 20 minutes at 300N thrust for the Arrow AUV, and 7 minutes at 67N thrust for the Arrow-Mini. While these are rather short times it was considered enough for conduction of experiments, which usually will not require sustained maximum thrust.

The control method for the vehicle is thrust vectoring, where the whole thruster assembly gimbals with two degrees of freedom. This method is used by a number of AUV systems (such as [7], [4]) and offers best performance regarding agility. Its integration into a confined, small hull envelope was a major challenge, since typical strategies such as linear actuators are not available in the required dimensions. The selected solution utilizes two watertight housed servos (SER2020 by Bluetrail Engineering) located in the tail section of the AUV. These

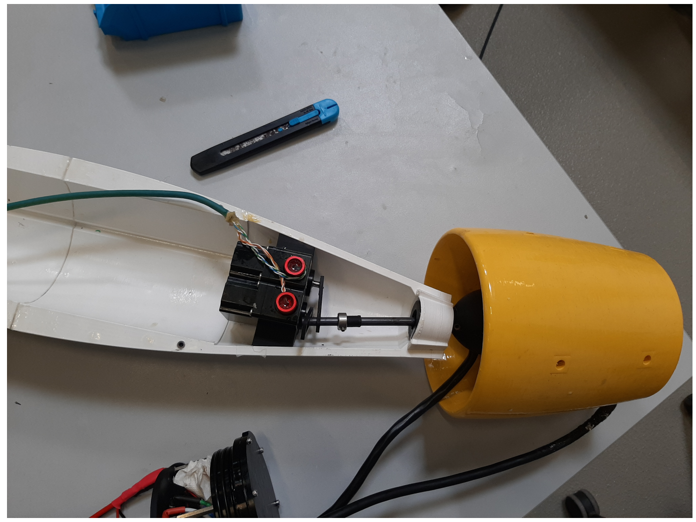

Fig. 3. Image of the vectoring mechanism in the tail section.

servos each have a hollow rudder horn attached, which are controlled in such a fashion, that they always overlap (see figure 4). Into this overlapping section the control rod with the thruster assembly is inserted. (see figure 3). The control rod is seated at the tip of the tail with a ball joint and directly attached to the thruster assembly. By variation of the length of the two parts of the lever (ball-joint to thruster and ball-joint to rudder horn) the forces at the servos can be managed even for large thruster forces. The resulting vectoring mechanism allows for a nearly symmetrical envelope of $\pm 7°$ in yaw direction and $-5 - 10°$ in pitch direction.

B. Electronics

All the electronics needed to fit into the rest of the pressure housings. Due to the complexity of miniaturizing the electrical systems the integration of the small version was paused at this point in order to gather experience with the full-sized Arrow AUV. For control a small computer (RaspberryPI CM4) was selected, its small size ideal for this application. For basic driving a microcontroller would have been sufficient, but for autonomy and (planned for later) sensor integration a full computer running ROS2 is more convenient. The CM4 is a scaled-down version of the popular Raspberry PI4b with limited peripherals but full access to the 40 pin GPIO header used for access to the board's communication interfaces.

Initially it was planned to use the BlueESC500 by BlueRobotics (sold together with the T500 thruster) as electronic speed controller. While it was initially integrated and tested, it lacks a feedback channel reporting RPM and other key values needed for autonomous operation of the vehicle. Consequently they were replaced by two VESCmini ESCs, which can be connected over a serial port and provide RPM as well as motor voltage and current. These again were replaced at a later stage by larger VESC5.3 ESCs, which have the same firmware but can provide up to 100A of current (the VESCmini are limited to 30A).

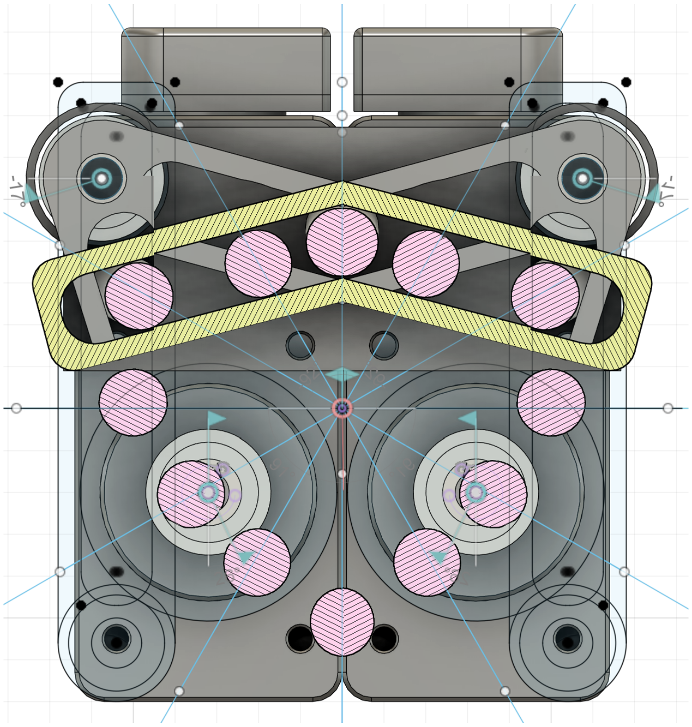

Fig. 4. Two servos of the vectoring mechanism showing their workspace as overlay. The magenta dots represent the position of the control rod in different rudder-horn positions.

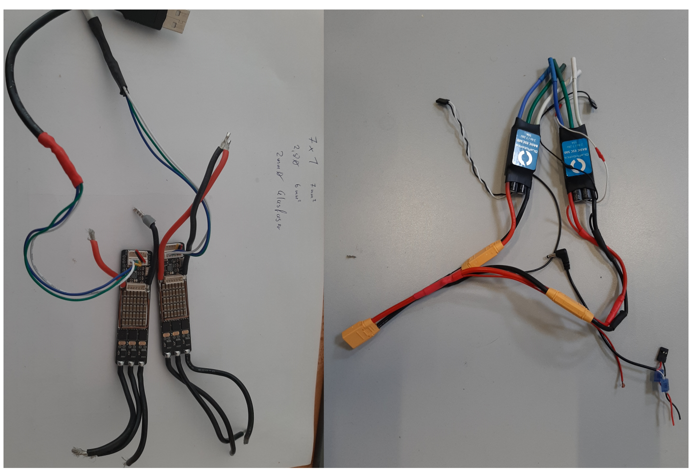

Fig. 5. Different options for electronic speed control of the thrusters: left VESCmini, right BlueESC500.

For navigation of the AUV an AHRS sensor was required. A MicroStrain 3DM-CV7-AHRS system was selected, due to its compact size, integrated Kalman filter and good performance specifications. It is connected to the control pc using a USB connection with the option of changing this to a serial connection later. One of the main selection criteria for the sensor was the fact, that a ROS2 library for it is provided by the manufacturer. For depth control a pressure sensor is integrated into the rear cap of the pressure hull, a Bar30 sensor by BlueRobotics. It is directly connected to the I2C port of

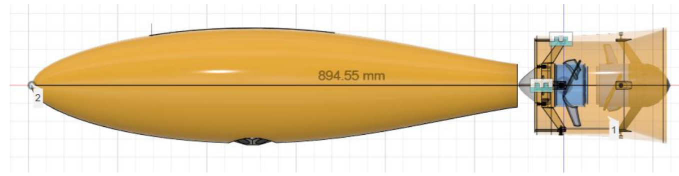

Fig. 6. CAD drawing of the Arrow AUV.

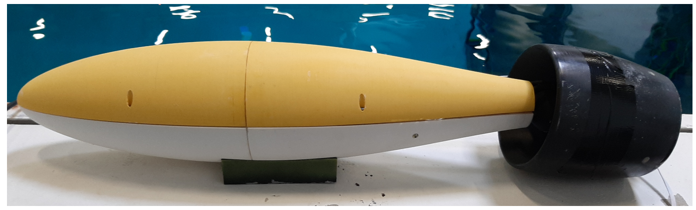

Fig. 7. Integrated Arrow AUV prior to tests in the basin.

the control PC. Initially it was planned to also integrate a Waterlinked A50 DVL into the system and in early CAD drawings it can be seen to fit into the vehicle (see figure 6). After performing CFD simulations and discovering the possible speed of the vehicle, the integration of this sensor was postponed since its maximum measurement velocity of 3.75m/s.

A complete CAD drawing of the vehicle is shown in figure 6, the insides of the pressure vessel are shown in figure 8 and the integrated vehicle can be seen in figure 7.

C. Software

The CM4 main PC runs an Ubuntu Server 24.04 linux with a ROS2 workspace. The PC can be programmed by a fiberoptic cable attached to the system as well as a WiFi connection (the latter only on land). Each sensor (AHRS, Pressure) and actuator (servos, thruster) has its own node, with a control node collecting all information from the sensors and sending control commands to the actuators. If a cable is attached it is also possible to control the AUV remotely with a joystick. The power consumption with all software components and sensors

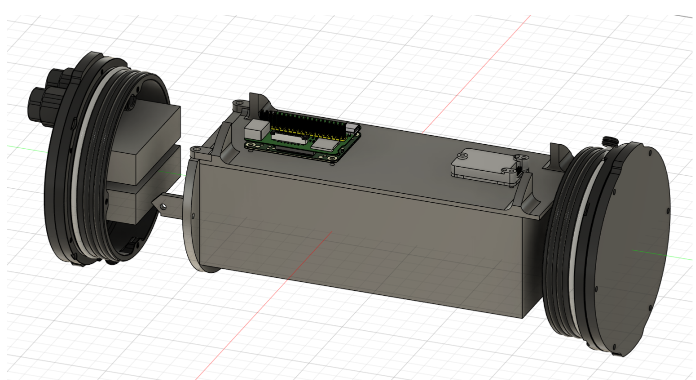

Fig. 8. CAD drawing of the insides of the pressure vessel. On the left side are the two ESCs (with room for cabling), the PI CM4 and the AHRS on top and the large battery occupying most of the space.

active is 4W and thus negligible in comparison to the 1500W peak power of the thrusters.

IV. Manufacturing

The hydrodynamically optimal hull is one of the most complicated components to manufacture, there are no COTS versions available, since it is so vehicle specific. Therefore two different manufacturing methods were investigated: The first, conventional method was milling the form of the hull from rigid foam using a CNC mill and subsequently strengthening it by applying a coat of fiberglass on top, after which it gets smoothed and painted. The second process involves the utilization of a FDM 3d printer and was discovered as feasible method during this work.

The conventional process of manufacture involves the milling of a rigid foam material by a CNC mill. The foam is selected considering required mechanical stability and buoyancy. For this work two different foams were used: Last-A-Foam R3312 by General Plastics with a density of 0.192 g/cm^3 as well as XPS foam with 0.03 g/cm^3. The first is much sturdier, but much more expensive and harder to mill. The latter is very brittle in its raw milled form but readily available from most hardware stores. The milling process involves the generation of two toolpaths, one for the inner side of the hull and a second one for the outer side. For the outer side the pre-milled blank was glued to a wooden spoilboard, which was later removed. The milling process is shown in figure 9. After milling the foam core requires an outer strengthening member in the form of a coat of glass-fiber reinforced epoxy. A single layer of glass fiber was cut and placed over the core. The assembly was placed in a vacuum bag and the expoxy vacuum-infused into the reinforcement (see figure 10). This method was chosen since it results in the most uniform epoxy coat as opposed to manual lay-up techniques. After curing the resulting hull segment was sanded and coated with a second layer of epoxy, which in turn was sanded and polished again to obtain a sufficiently smooth and rigid hull segment (see figure 11). Since the main strength member in this process is the curved glass fiber reinforced epoxy, no significant differences (apart from the weight) were aparent between the two different types of foam. The results are very lightweight (R3312: 0.29g/cm^3, XPS: 0.13g/cm^3), rigid hull segments which perform very well in an underwater environment. The downsides of this process are the requirement of specialized machinery (CNC mill, vacuum infusion equipment) as well as handling of hazardous material and a lot of manual work, approximately 12 hours of work and numerous curing breaks.

While the initial hull was machined using the process described above, the thruster nozzle was 3d printed (using a FDM process) for functional testing. Since its shape would have been complicated to mill, requiring a 6 axis mill, methods for making the 3d printed part fit for use underwater were investigated. One typical method for this is printing with 100% infill settings, making the part solid and thus watertight. Unfortunately this would result in a very heavy tail section, since the thrusters are already more dense than water. Simply

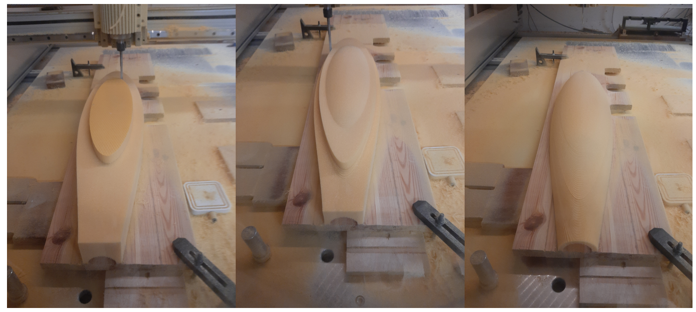

Fig. 9. Manufacturing process of milled hull half.

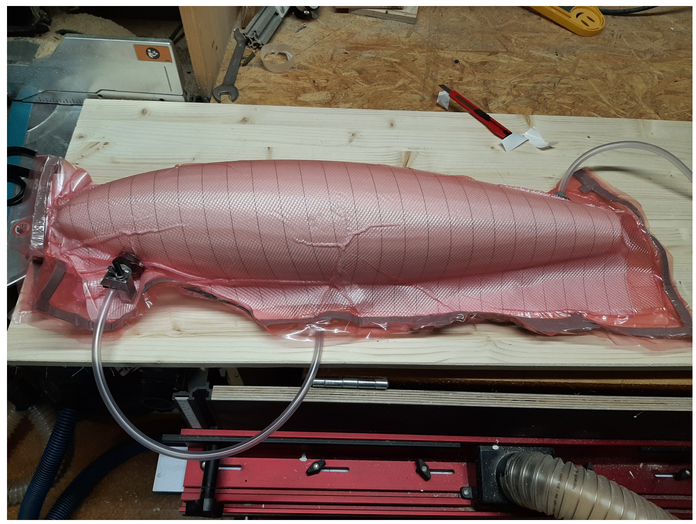

Fig. 10. Resin infusion of milled hull.

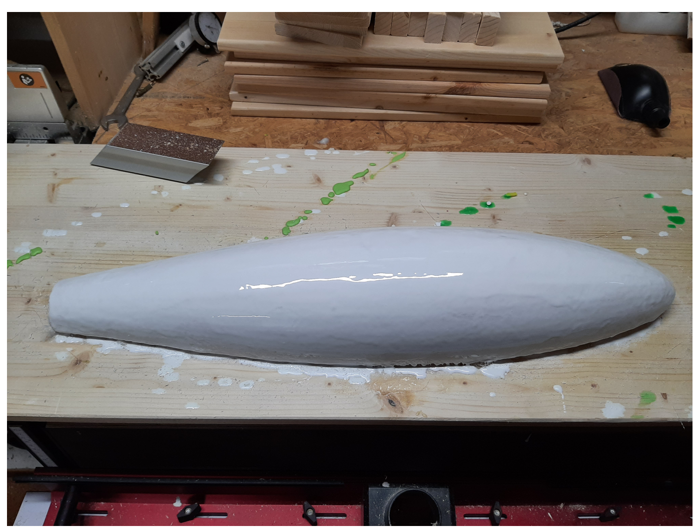

Fig. 11. Coating the fiberglass reinforced hull blanks with a layer of UV-resistant epoxy.

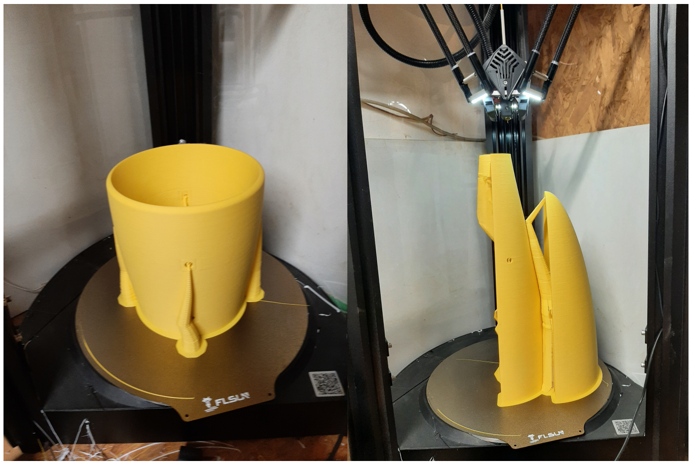

Fig. 12. Manufacturing process of 3d-printed hull and nozzle.

3d printing with a lower infill ratio (resulting in a hollow, less dense part) would not work, since during the FDM process watertighness of the individual layers cannot be guaranteed. There are a number of methods for making FDM-3d-printed parts watertight, all involving either coating the part or infusing it with a sealing agent. To the author's knowledge none of these methods was used in the past for creating buoyant underwater components, and the selected method and various results with it have been published in a paper in Oceans 2024 Halifax (no citation available, currently in processing). A short summary of the process is the following: the buoyancy component is exported from CAD to a slicing program, where it is sliced with 10% infill, 3 walls and additional strength members at physical attachment points. After printing with a reasonably tuned 3d printer (material for this work was PLA, but other materials have been investigated in the aforementioned paper) the resulting component is infused with a sealing agent (Diamant dichtol AM Hydro) by submerging the part in the sealing agent and subsequent drying. The resulting part is low-density (e.g. upper hull: 550g weight with a volume of 1.688l, resulting in a density of 0.32 g/cm^3) and watertight at least for 100m submersion. While not achieving the performance concerning density or rigidity of the milled hull segments described above, the overall process is fairly straightforward, only requiring a 3d printer and some (unsupervised) printing time. Total time required for a single-side hull segment was 14 hours of 3d printing, 30 minutes of submersion in the sealing agent and 12 hours of curing, resulting in only approx. 1 hour of manual work required per hull segment. Since this process worked so well for the thruster nozzle it was later also adopted for the hull segments of the vehicle, depicted in figure 12.

V. Discussion

A CFD analysis was conducted to assess the vehicle's performance characteristics. The Open-Source CFD toolbox "'OpenFoam"' was used for this, and the CAD-model of the vehicle was used to compute the resulting forces for water speeds of 1-15$\frac{m}{s}$. The results can be seen in figure 13. At 14$\frac{m}{s}$ the resulting force reaches 293N, which would be the maximum thrust of the coaxial thruster. Since the datasheet value for the thrusters is bollard-thrust, a realistic value for top speed is assumed to be 12$\frac{m}{s}$, where a force of 216N has to be generated by the thrusters. This would lead to a maximum distance of 14.4km the vehicle can travel at full thrust in 20 minutes.

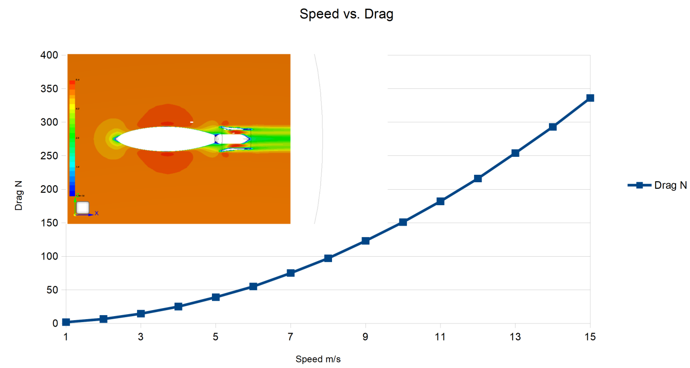

Fig. 13. CFD simulation of Arrow-AUV with speeds from 1-15$\frac{m}{s}$.

One of the aims of this work was to create a vehicle with as many COTS components as possible. This goal was reached: all components, safe the hull, are COTS components. Of course there is a certain amount of assembly and tools required for the electronics integration, but with a simple electronics workshop (soldering iron, wire, shrink tube) this is no hindrance. The hydrodynamic hull and thruster shroud are printed on a fairly standard 3d printer, which is available for as little as 200$ and requires minimal special skills. The only component which requires specialized machinery is the rudder horns, which failed multiple times as 3d printed models - in the end they had to be watejet-cut from carbon-fiber-composite material in order to work properly. This however can be achieved by placing a custom order for these components either from a local machine shop or an online service. The resulting system can be replicated for a total cost of approx. 4000$, which is at the lower end for an autonomous underwater vehicle.

VI. Results

The "Arrow" AUV system has a weight of 7kg and a peak thrust of 300N, resulting in a thrust-to-weight ratio of 4,37. This is a significant improvement over other AUV systems. After the integration of the AUV a number of experiments have been conducted in the test basin at the DFKI-RIC in Bremen. While the first experiments looked at the overall viability of the concept, trials measuring peak speed, roll stability, maneuverability and autonomous control have been conducted. A maximum velocity of 7$\frac{m}{s}$ could be measured but this was limited by the size of the test basin (23x19m). The measurements have been conducted by manual evaluation of images taken by an underwater camera. Additional trials at a lake are scheduled for larger-scale tests. The roll stability is

Fig. 14. Different versions of hulls in comparison. On the lower hull 3d tracking markers are visible.

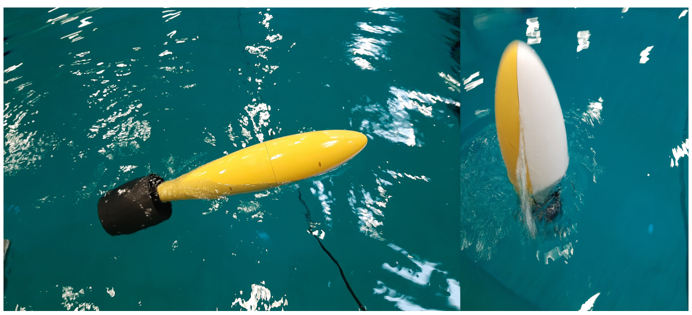

Fig. 15. Arrow AUV in the water and jumping.

excellent with the two thrusters rotating in opposite directions. If operated at slightly different RPM a torque can be applied to the system, actively controlling the roll position of the vehicle. This has only been tested with manual controls, but a simple controller using the input from the AHRS should be able to stabilize the vehicle in arbitrary roll configurations, which might be interesting for future applications.

A number of possible applications for such vehicles have been identified, of particular interest are areas where fast response is paramount (e.g. search+rescue) as well as operation in strong current environments.

During the work with the Arrow AUV a number of different hulls and nozzles have been produced and tested. Most of these were slight modifications and optimizations but there were also some necessary replacements due to damage (from collisions/jumping).

One problem encountered early on was the tendency of the fiberoptic cable (used for remote control) being sucked into the thruster, resulting in damage to both the thruster and the cable. This could be remedied by utilization of a stiffer fiber and attaching the fiber to the thruster nozzle with tape (see figure 16).

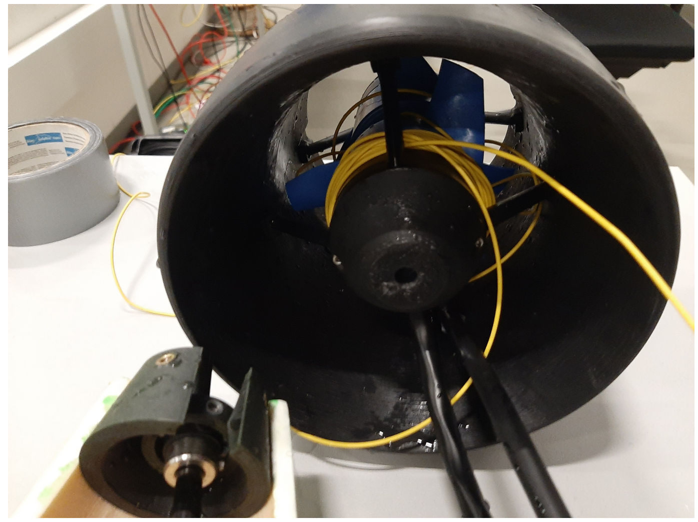

Fig. 16. Fiberoptic communication cable caught in thruster.

VII. Future Work

There are a number of planned experiments and modifications with the system. Apart from outdoor trials to measure maximum speed, the ability of the vehicle to jump out of the water and re-enter in a controlled manner will be researched. In the test basin its ability to jump could already be demonstrated, however for controlled re-entry more investigation and controller tuning is required. Another planned experiment is inverse-pole-balancing, where the vehicle stands upright in the watercolumn controlling its position using its vectoring mechanism. Since the underwater test basin at DFKI is equipped with a camera-based tracking system (Qualisys), more comprehensive measurements of the vehicle speed and its maneuverability while being tracked will be conducted. One of the planned modifications is the integration of a camera for recording of visual video as well as the aforementioned DVL sensor. A future quality-of-life modification will be the addition of a charging port, removing the necessity of opening the pressure vessel in order to replace the battery.

References

[1] J. Albiez et al. Flatfish - a compact subsea-resident inspection auv. In *OCEANS 2015 - MTS/IEEE Washington*, pages 1–8, 2015.

[2] B. Allen, R. P. Stokey, T. C. Austin, N. C. Forrester, R. G. Goldsborough, M. Purcell, and C. von Alt. Remus: a small, low cost auv; system description, field trials and performance results. *Oceans '97. MTS/IEEE Conference Proceedings*, 2:994–1000 vol.2, 1997.

[3] S. Bhat. Hydrobatics: Efficient and agile underwater robots. Master's thesis, KTH, School of Engineering Sciences, 2020.

[4] T. Creutz, B. Wehbe, S. Arnold, and M. Hildebrandt. Towards robust autonomous underwater docking for long-term under-ice exploration. In *OCEANS 2023-Limerick*, pages 1–8. IEEE, 2023.

[5] D. J. S. H. N. Arafat and W. L. Neu. Development of a dynamic model of a small high-speed autonomous underwater vehicle. In *OCEANS 2006, Boston*, OCEANS, pages 1–6, 2006.

[6] M. Hildebrandt, J. Albiez, M. Fritsche, J. Hilljegerdes, P. Kloss, M. Wirtz, and F. Kirchner. Design of an autonomous under-ice exploration system. In *2013 OCEANS-San Diego*, pages 1–6. IEEE, 2013.

[7] S. Willcox, D. Goldberg, J. Vaganay, and J. Curcio. Multi-vehicle cooperative navigation and autonomy with the bluefin cadre system.